SURFACE REPAIRS BY MMAW AND MIG - INFLUENCES ON FRACTURE ENERGY

R. CIOCOIU [1], N. NAVODARIU[1], A. DINITA [2], O. TRANTE[1*], C. MILEA[1], I. CIUCA[1], R. COMAN[1], V. SACELEANU[3]

The aim of this study was to determine which weld repairing method of cavitation/erosion damage of stainless steels would ensure a good toughness. Sets of specific specimens were obtained and manual metal arc and metal inert gas weld repaired and tested by Charpy pendulum impact tests. Additional hardness measurements were performed on the weld metal and heat affected zone.

A finite element analysis was performed on a simplified model to find stress distribution in an assembly with various characteristics.

Main influence factor on the toughness was welding heat input by altering the microstructure of the heat affected zone.

1. Introduction

Cavitation and erosion are the main damage mechanisms of submerged water turbine components [1]. Cavitation is a phenomena that appears in a flowing system when the static pressure goes below the vapor pressure of the liquid - vapor bubbles form. By collapsing near materials pitting or surface erosion of the component results affecting the long run by failure [1, 2]. Failure analysis is performed today for various industrial cases, in order to elucidate the failure mechanism and develop potential solution to prevent the failure [3-7].

Cavitation and erosion damage of submerged components are usually performed in situ by filling the pits with welding. Some water turbine blades maintenance guides recommend repairs using welds of cavitation or erosion features deeper than 3mm.

Stainless steels are readily joined by arc welding preferably under controlled conditions [8, 9]. Manual metal arc welding is a metal arc welding process that uses a consumable electrode covered with a flux. An electric arc is created between the electrode and the base metal creating a pool of melted metal which, when cooled, forms a joint. The flux disintegrates and creates a shielding gas and slag that protects the weld area from the atmosphere. In metal inert gas

[1] Materials Science and Engineering Faculty, University POLITEHNICA of Bucharest, Romania,
* O. Trante as corresponding author, e-mail: tranteoctavian@yahoo.com
[2] *Petroleum - Gas* University of Ploiesti, Romania
[3] University *L. Blaga*, Sibiu, Romania

welding an electric arc is formed between a consumable wire electrode and the base metal creating a molten pool of metals which, when cooled, creates a joint.

Welding of martensitic stainless steels requires attention: the heat affected zone becomes susceptible to cracking and usually pre- and post-heating treatments are required. Microstructure transformations are affected by welding heat input: high heat inputs result in slow cooling rates

If the heat input "*H*" is an arc it depends on voltage "*U*", intensity "*I*" and the travel velocity of the heat source "*v*" according to equation (1).

$$H = \frac{U \cdot I}{v} \tag{1}$$

If the martensitic stainless steels are heated above the critical temperature a fully austenitic microstructure appears which upon cooling rapidly below transformation temperature transforms back to martensite. Melting temperatures for this type of steels are in the range of 1500C with less heat conductivity than mild steels (depending on temperature range) and general weld procedures are dictated by carbon content: if the carbon content is less than 0.10% no preheating or post weld heat treatments are required. When preheating is required it is advisable to be performed in the 200 - 350°C range.

The use of stainless-steel filler metal is advisable to prevent brittle welds. Ductile weld metals are preferable but hardening in the heat affected zone remains a problem.

The experiments performed within this study aim to determine the fracture energy of two different welding techniques manual metal arc and metal inert gas applied on a cast martensitic stainless steel.

2. Materials and Methods

The base metal is obtained from a discarded water turbine blade which was cut into several specimens, five with approximately equal dimensions (150x60x15mm) were selected and further processed by machining a 3mm deep grove (on average), as shown in Fig. 1.

The groove simulates cavitation and erosion damage and it is repaired, as the conventional procedure recommends, by weld filling using 316L stainless steel as weld material using two welding methods: manual metal arc welding (MMAW) and metal inert gas (MIG) welding. Two specimens were used for each welding procedure: one at room temperature designated as "cold sample" and one preheated at 400°C designated as "warm sample". A fifth sample was used as reference and no processing was performed on it. Sample coding and processing is presented in table 1.

Table 1

Sample coding and processing

SAMPLE CODE	WELDING METHOD	PREHEATING
P1	MMAW	NO.
P2	MMAW	YES, 400C.
P3	MIG	NO.
P4	MIG	YES, 400C.
NS	REFERENCE.	NONE.

The welding parameters were adapted to sample dimensions, electrode/wire diameter, heat source travel speed, arc current voltage and intensity. Equation (1) was used to determine the heat input and for MMAW was found at 290.73kJ/mm and for MIG at 822.96kJ/mm. The heat input in MIG welding is 2.83 times higher than by MMAW welding which should create problems in the heat affected zone.

The first analysis performed was to determine the chemical composition of the base metal by optical emission spectrometry using the SPECTROMAXX optical emission spectrometer.

Preheating of the samples was performed in a Nabertherm LE6/11 electric furnace with heating temperature of 400°C and a holding time of 2 hours.

The hardness measurements were performed on a HRC hardness tester from Balanta Sibiu, Romania.

From the weld repaired samples Charpy specimens with dimensions according to SR EN ISO 148-1:2011 were obtained and tested using a Walter+Bai Charpy pendulum with a nominal energy of 300 J; fractured specimen investigation was performed by macroscopic examinantion and using a Scanning electron microscope Hitachi – S3400N/Type II.

A load transfer study was performed using the SolidWorks Simulation module within Dassault Systems SolidWorks software.

3. Results and discussion

In table 2 the chemical composition of the steel is presented. Since little variation on alloying element concentration was observed, the mean values of 12 measurements is presented.

Table 2

Chemical composition of the steel

Element	C	Si	Mn	Cr	Ni	Mo	Cu	Fe
%wt	0.08	0.24	0.441	13.44	1.59	0.065	1.18	Bal.

The chemical composition of the stainless steel was found to be a 10Ch12NDL casting stainless steel according to GOST 977 /988.

The Charpy impact tests specimens conformed to ISO 148-1 dimensions. The schematic in Fig.2 shows the configuration for the test where the weld repaired region opposes the V notch.

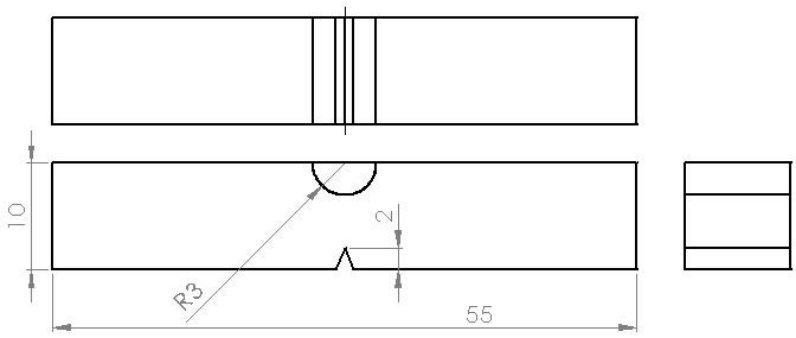

Fig. 2 Weld repaired Charpy impact specimens

The hammer impacts the region where the weld material was deposited. Three samples were tested/specimen type and the confidence intervals for the mean in this entire study are reported at a significance level α=0.05.

The fracture energy results are shown in table 3.

Table 3

Fracture energy results obtained by testing 3 specimens

Sample	Average [J]	Standard deviation [J]	Mean confidence interval
P1	65.33	4.12	4.66
P2	110.80	4.55	5.15
P3	30.57	3.93	4.45
P4	32.23	7.58	8.58
NS	92.40	1.35	1.53

Analyzing the variation of fracture energy presented in Fig. 3 it can be seen that by MIG welding very low values are obtained, while using MMAW higher values, sometimes higher than the base material were obtained.

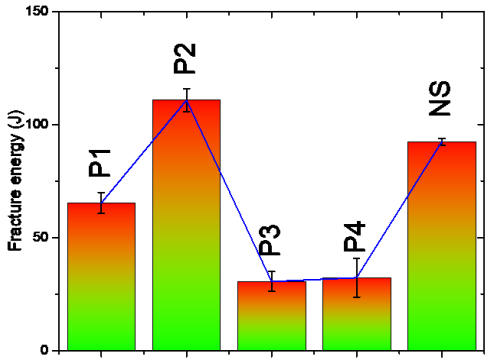

Fig. 3 Variation of fracture energy showing confidence intervals for the mean

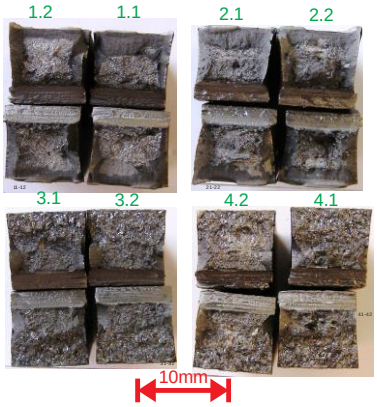

Fig. 4 Fracture surface of tested specimens showing a mixed mode of fracture

The MIG repaired samples are brittle and preheating shows little influence on the fracture energy. The MMAW welded specimens show considerable larger values, the cold samples have inferior values when reported to the reference, but the warm specimens supersede the reference by approximately 30J.

The next study involved fracture surface investigation and Fig. 4 shows a selection from the weld repaired and tested specimens. Generic observations revealed a mixed mode of fracture where areas with specific brittle and ductile features are present. Using Image-Pro Plus v. 6.0 the areas with ductile appearance were measured on images similar to those shown in Fig. 4.

Using the procedure described above the analysis was performed on each tested samples and the mean values are shown in table 4.

Table 4

Percent surface area with ductile appearance

Sample	Average [% area with ductile appearance]	Standard deviation [% area with ductile appearance]	Confidence interval of the mean
P1	53.33	2.47	2.79
P2	71.50	0.76	0.86
P3	10.96	2.92	3.31
P4	12.00	4.48	5.07
NS	56.30	0.97	1.10

In Fig. 5 the variation of the data presented in the previous table is presented: samples repaired by MMAW show similar values to reference samples NS, while MIG repaired specimens show a 5 times less percent area with ductile appearance.

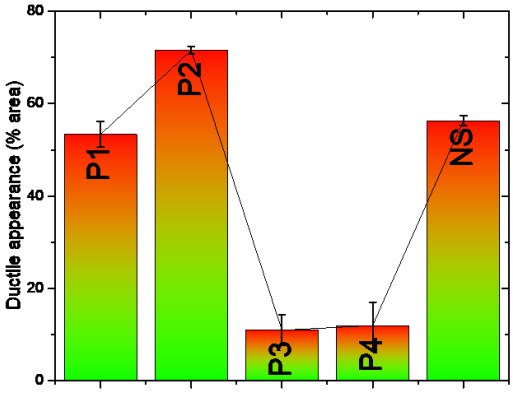

Fig. 5 The percent surface area with ductile appearance on fractured specimens

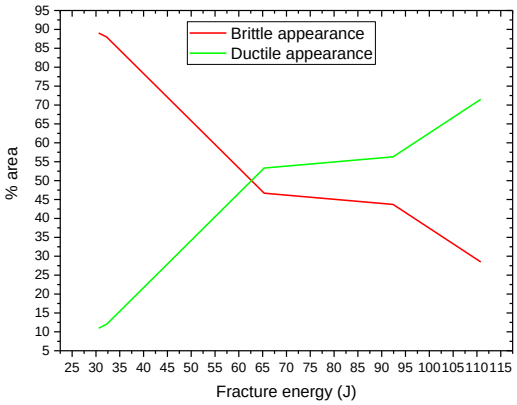

Fig. 6 The %area of ductile and brittle appearance variation in respect to the fracture energy

On the warm samples when using MMAW an increase of ductile fracture area was observed, while on MIG welded samples no statistical significant variation was found.

The ductile and brittle appearance in respect to fracture energy variation is shown in Fig. 6. As expected, when fracture energy increases the %area brittle appearance decreases and the ductile one increases.

The hardness test were performed on all samples along the welded region (on the weld metal), adjacent to it on the heat affected zone (HAZ) and on the reference sample. The hardness results for weld material (Fig. 7.a) and HAZ (Fig.7.b) are compared with the reference sample (NS).

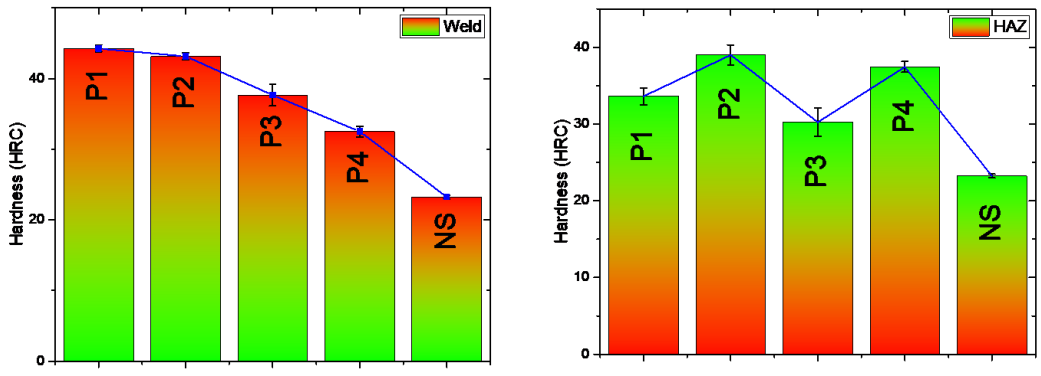

a. b.

Fig. 7 Hardness mean values on a. weld metal and b. heat affected zone and the reference sample, NS

According to Fig. 7.a when MMAW welding is used the hardness reaches its largest values and sample preheating showed no statistical significant difference when we compared the cold and warm mean values.

When MIG welding was employed the warm sample showed a decrease in hardness when compared to the cold sample.

In Fig. 7.b the hardness of the HAZ was found to vary in a similar manner on both MMAW and MIG welded samples: the warm samples showed increased hardness than that of the cold samples and higher than the base metal.

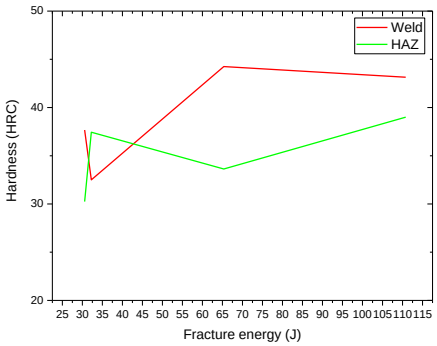

Fig. 8 Hardness variation of the weld metal and heat affected zone as fracture energy increases

A variation of hardness in respect to fracture energy of both weld materials and HAZ is plotted in Fig. 8.

As higher fracture energies were reached, the HAZ hardness showed an increase while the weld metal hardness showed a decrease.

The scanning electron microscopy studies performed on the fracture surface revealed further details of the fracture morphology.

In Fig. 9 details from the fracture surface of one from the P2 specimens which achieved a 116J fracture energy are shown.

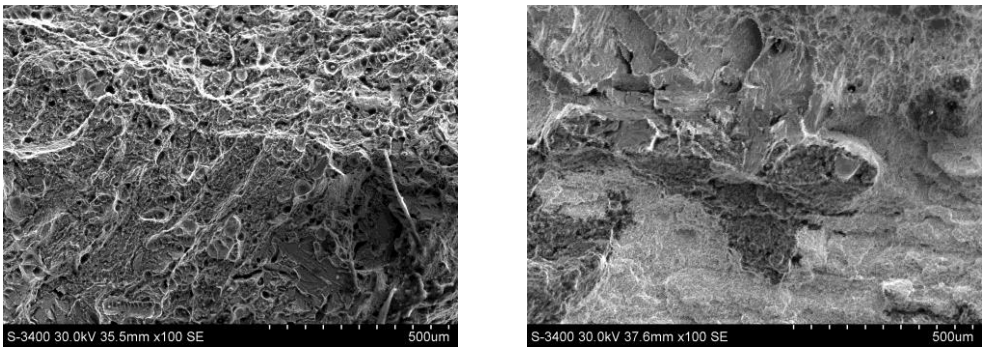

Fig. 9 Scanning electron microscopy images of the fracture surface on a sample from the P2 series

A ductile, fibrous fracture morphology is dominant and at higher magnification dimples with voids are observable. In Fig. 10 brittle fracture characteristics are dominant; the sample stems from P3 specimens with a 35J fracture energy recorded.

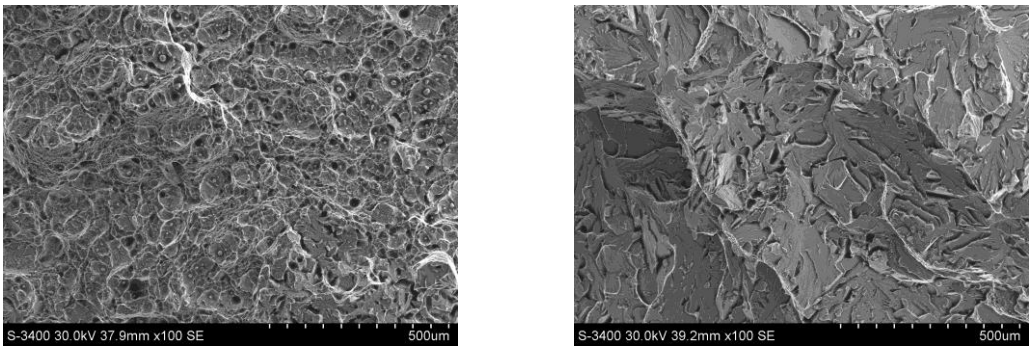

Fig. 10 Scanning electron microscopy images of the fracture surface on a sample from the P3 series

Obviously, the fracture was not completely brittle; regions with dimples were also observed. Spherical precipitates appear in the dimples observed in Fig. 10, while no such precipitates were observed in those shown in Fig.9.

The results obtained by current studies would suggest that using MMAW higher fracture energies can be achieved when the base metal is preheated which can be explained by changes in microstructure.

Microstructure change impacts on mechanical properties, a reason to continue with further studies using SolidWorks Simulation to observe how these microstructure changes in various volumes determine the stress distribution within the assembly.

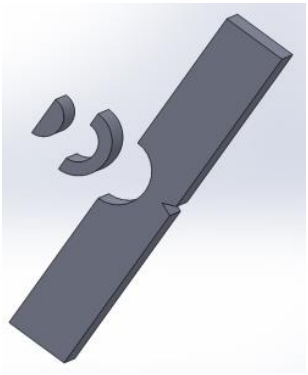

Fig. 11 Simplified model showing the three volumes. From left to right: weld metal, heat affected zone and base metal.

From a mechanical point of view load transfer was studied using a simplified model shown in Fig. 11. The sample was devised in 3 volumes: first volume was the weld material, the second volume the heat affected zone and the third volume the base material.

The materials in the study have specific parameters to fit the intended scenario and do not correspond necessarily to real materials. Two scenarios were studied where the mechanical characteristics of the weld metal were modified. Study 1 comprises materials with similar yield strengths and deformations at failures while in study 2 the weld metal is considered more plastic, with lower yield strength, elastic modulus and higher deformation at failure.

The load was applied on the weld material and the results obtained were studied by observing the Von Misses stress distribution (Fig. 10) and the strain (Fig. 11).

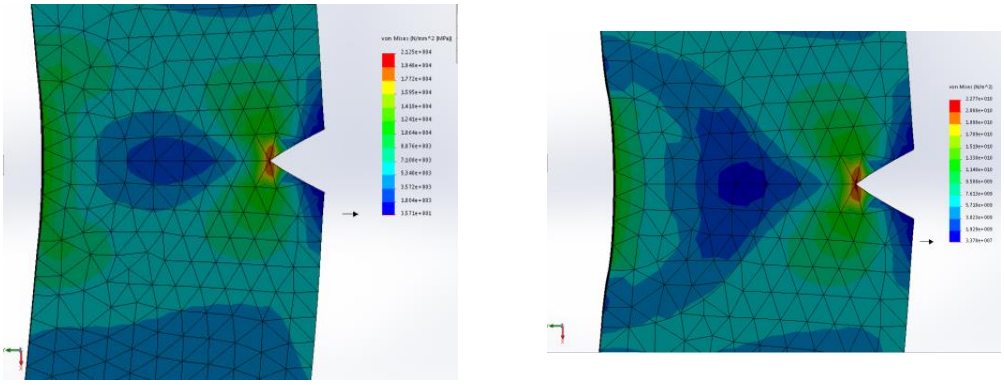

a. b.

Fig. 10 Von Misses stress distributions on a. an assembly with similar material properties and b. an assembly with a more ductile weld metal

When the materials for all volumes were similar in characteristics the stress distribution is shown in Fig. 10.a. The load is transferred through the sample, while in Fig. 10.b, when the weld material is more ductile, a completely different stress distribution is seen where the weld metal should absorb more energy and deform.

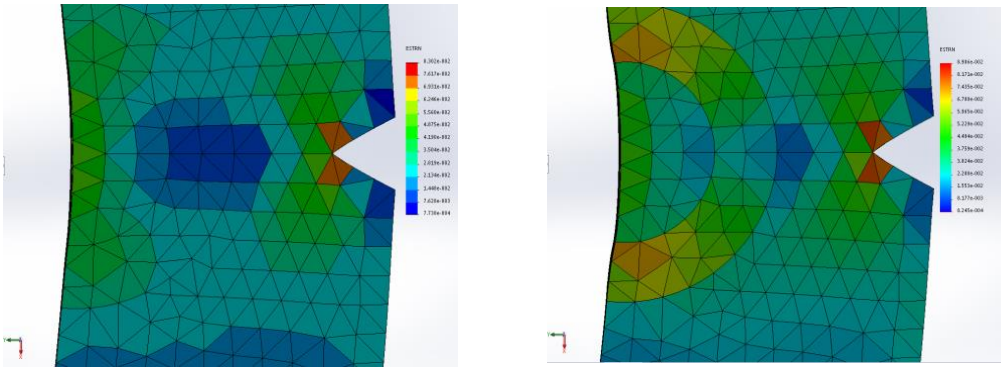

a. b.

Fig. 11 Strain distributions on a. an assembly with similar material properties and b. an assembly with a more ductile weld metal

The strains obtained confirm that when materials of all volumes are similar strains are almost uniformly distributed as seen in Fig. 11.a, while dissimilar characteristics can create different strains within the ensemble, as depicted by Fig. 11.b, where the weld metal deforms and absorbs more energy.

4. Conclusion

High heat inputs generated when MIG welding creates deleterious microstructures and lower assembly toughness. Sample preheating showed no influence on the fracture energy. Lowering the heat input, by MMAW, the resulting microstructures became more favorable to promote toughness and preheating shows a significant influence since the samples showed a fracture energy higher than the base metal. High energy inputs reduce the heat affected zone toughness.

Individual volume mechanical characteristics (weld metal and heat affected zone) are also important for stress distribution and assembly toughness: as the weld metal volume is less stiff, it absorbs more energy and deforms plastically.

This study showed that the toughness of the assembly is mainly governed by microstructure changes which occur by heating. Different volume heating generates various microstructures with specific mechanical properties which impacts on the stress distribution and on the load transfer, inherently affecting the fracture energy.

R E F E R E N C E S

[1] B. K. Sreedhar, S. K. Albert, et al. (2017). "Cavitation damage: Theory and measurements - A review." Wear **372**: 177-196.

[2] B. Ghiban, I. Bordeasu, et al. (2008). "Some Aspects of Cavitation Damages in Austenitic Stainless Steels." Annals of Daaam for 2008 & Proceedings of the 19th International Daaam Symposium: 541-542

[3] M. Bane, F. Miculescu, et al. (2012). "Failure analysis of some retrieved orthopedic implants based on materials characterization". Solid State Phenomena **188**: 114-117.

[4] R. Marinescu, I. Antoniac, et al. (2017)."Clavicle anatomical osteosynthesis plate breakage - failure analysis report based on patient morphological parameters." Romanian Journal of Morphology and Embriology **58(2)**:593-598.

[5] D. Grecu, I. Antoniac, et al. (2016). "Failure analysis of retrieved polyethylene insert in total knee replacement." Materiale Plastice **53(4)**:776-780.

[6] M. Rivis, M. Pricop, et al. (2018). "Influence of the Bone Cements Processing on the Mechanical Properties in Cranioplasty, "Revista de Chimie **69(4)**:990-993.

[7] I. Antoniac, M. Negrusoiu, et al. (2017). "Adverse local tissue reaction after 2 revision hip replacements for ceramic liner fracture A case report, ."Medicine **96(19)**:e6687.

[8] M. Sohaciu, S. Ciuca, et al. (2016). "Influence of turbine blades fabrication conditions on their lifetime." Optoelectronics and Advanced Materials-Rapid Communications **10(3-4)**: 257-261.

[9] G. Coman, S. Ciuca, A.C. Berbecaru, M.C. Pantilimon, M.G. Sohaciu, C. Gradinaru, et al., (2017) "New Martensitic Stainless Steel Hardenable by Precipitation for Hydropower Turbines", Univ Politeh Bucharest **79**:209-18.